

Identification of four functional NR3B isoforms in developing white matter reveals unexpected diversity among glutamate receptors

António M. de Jesus Domingues,^{*†} Karla M. Neugebauer[†] and Robert Fern^{*}

^{*}Department of Cell Physiology and Pharmacology, University of Leicester, Leicester, UK

[†]Max Planck Institute of Molecular Cell Biology and Genetics, Dresden, Germany

Abstract

Functional neurotransmitter receptors are expressed in central white matter, where they mediate ischemic damage to glia and may be involved in cell–cell signalling. In this study, we analysed NMDA receptor NR1, NR2B-C and NR3A-B subunit expression in the brain and optic nerve by molecular cloning. In addition to the canonical forms of NR1 and NR2, four previously unknown NR3B variants, generated by alternative splicing, were identified. The variants encoded for isoforms with deletions of 8/15 amino acids in the N-terminal domain or 200/375 amino acids removing one or three transmembrane domains and part of the C-terminal domain, as compared with the previously charac-

terized NR3B isoform. Co-expression of NR3B isoforms with NR1/NR2A-C modulated the amplitude and Mg²⁺-sensitivity of glutamate responses in a NR2 subunit-dependent fashion, with significant variations in the effects produced by different isoforms. These effects were not the result of reduced surface expression of the receptor complex since all NR3B isoforms reduced surface expression by a similar degree. These data reveal previously uncharacterized regulation of NMDA receptor function by alternative splicing of the NR3B subunit.

Keywords: glia, glutamate, NMDA, neurotransmitter, splicing isoform, white matter.

J. Neurochem. (2011) 10.1111/j.1471-4159.2011.07212.x

Pre-synaptic release of neurotransmitters and subsequent detection by specific post-synaptic receptors is used throughout the CNS to mediate information transfer and integration. Once thought to be the *sine quo non* of neuronal function, it is now known that synapses also form between neurons and glia. Glutamatergic post-synaptic potentials have been recorded in NG-2(+) glia, astrocytes and oligodendroglia, in both grey and white matter regions of the brain (Paukert and Bergles 2006; Verkhratsky and Kirchhoff 2007). Although there is evidence that white matter glutamate and ATP receptors help to coordinate the complex morphological arrangement between glia and axons (Ishibashi *et al.* 2006; Alix *et al.* 2008), there is little information on the physiological properties of white matter receptors and it is not known if their molecular properties differ from receptors in grey matter. Despite this, there is growing evidence that white matter receptors are important in pathological conditions such as multiple sclerosis, spinal cord injury, stroke and cerebral palsy (Karadottir *et al.* 2005; Salter and Fern 2005; Micu *et al.* 2006; Alix and Fern 2009; Constantinou and Fern 2009; Nikolaeva *et al.* 2009; Ouardou *et al.* 2009a,b).

White matter receptors encounter lower neurotransmitter concentrations than occur at grey-matter synapses and appear to mediate tonic signalling rather than rapid signal integration (Kukley *et al.* 2007; Gallo *et al.* 2008). The best-studied example is the NMDA-type glutamate receptor that mediates post-synaptic potentials in astrocytes (Verkhratsky and Kirchhoff 2007) and oligodendroglia (Karadottir *et al.* 2005). In both cases, the receptor has low Mg²⁺-sensitivity and unique pharmacological properties that do not align with any known subunit stoichiometry. NMDA receptors are a class of ionotropic glutamate receptors important for mediating synaptic-transmission in grey matter. A functional NMDA receptor is composed by two NR1 subunits (obligatory subunit) and two NR2(A-D) subunits all coded in

Received December 6, 2010; revised manuscript received January 21, 2011; accepted January 21, 2011.

Address correspondence and reprint requests to Robert Fern, Department of Cell Physiology and Pharmacology, University of Leicester, PO Box 138, University Road, Leicester, LE1 9HN, UK.

E-mail: rf34@leicester.ac.uk

Abbreviation used: PBS, phosphate-buffered saline.

different genes. NR3(A-B) subunits can also be included in the receptor and are postulated to have a modulatory dominant-negative function (Low and Wee 2000; Cavara and Hollmann 2008).

Once thought to be absent from oligodendrocytes, it is now known that functional NMDA receptors are expressed in this type of glial cell and can mediate cell damage (Karadottir *et al.* 2005; Salter and Fern 2005; Micu *et al.* 2006). Although molecular and electrophysiological evidence suggests that these receptors might be composed of NR1/NR2C/NR3(A-B) subunits, their pharmacology is unique (Karadottir *et al.* 2005). We therefore wanted to test the hypothesis that NMDA receptors expressed in the white matter are novel at the molecular level because of the incorporation of new splicing isoforms that modify the receptors to subservise white matter functions that are distinct from neurotransmitter functions at neuronal synapses. For this purpose, we have cloned NR3B from the neonate rat optic nerve, a white matter tract, and present here the characterization of 4 previously unidentified splicing isoforms of this NMDA receptor subunit.

Methods

mRNA extraction and molecular cloning

Lister-hooded rats of both sexes aged between postnatal day 10 (P10) and P14 (called 'P10' throughout) were killed in accordance with the regulations of the British Home Office (animals bred in house). Optic nerves were excised and placed in phosphate-buffered saline (PBS). RNA extraction, reverse-transcription and detection of NMDA receptor expression by PCR was performed as previously described (Salter and Fern 2005). To generate full-length cDNAs, reverse transcription was performed on 1 µg of total RNA from either optic nerve or whole brain RNA using PowerScript (Clontech-Takara Bio Europe, Saint-Germain-en-Laye, France) and mRNA was primed with an oligo(dT)₂₄V primer. PCR was then performed with *LA-Taq* (Clontech-Takara Bio Europe, Saint-Germain-en-Laye, France) for the amplification of NR1, NR2A, NR2B, NR3A and NR3B. Because of the high GC-content of NR2C we used *LongRange PCR enzyme mix* with the *Q reagent* (Qiagen, Valencia, CA, USA) for the amplification of this subunit. Cycling condition can be found in Table S1. All primers are listed in Tables S2–S4. PCR products were then cloned in the pGEM-T vector and sequenced.

Construction of fluorescently tagged subunits

To create NR2C and NR3A-B tagged with fluorescent proteins, the coding sequence for NR2C, NR3A-B, EYFP and mCherry were PCR amplified (PfuUltra II Fusion HS DNA Polymerase; Stratagene, La Jolla, CA, USA) using primers containing restriction sites. The amplicons were cut with the appropriate restriction enzymes and ligated in the mammalian expression vector pcDNA3 (Invitrogen, Carlsbad, CA, USA), creating pcDNA3-NR2C-YFP (Yellow Fluorescent Protein), pcDNA3-NR3A-mCherry and pcDNA3-NR3B-mCherry. The constructs were sequenced to confirm sequence fidelity. Fluorescent tags are located at the

C-terminus of the subunits NR2C-YFP, NR3A-mCherry and NR3B-mCherry. NR1-CFP (Cyan Fluorescent Protein) (NR1-1a), NR2A-YFP and NR2B-YFP were tagged at the N-terminus (Qiu *et al.* 2005) and were a kind gift from Dr Jian-hong Luo (Zhejiang University School of Medicine, China). The plasmid coding for mCherry was a gift from Dr Roger T. Tsien (University of California, USA). Tagging of NMDA receptors subunits at both N- and C-terminus has been done in the past and tagged subunits form functional channels (Marshall *et al.* 1995; Smothers and Woodward 2003).

Cell culture and transfection

HEK293 cells (ATCC, CRL-1573) were grown in Dulbecco's modified Eagle's medium supplemented with 10% fetal bovine serum. Cells were plated on poly-L-lysine coated coverslips for calcium imaging or on uncoated 6-well plates for cell sorting and grown to ~50–70% confluence. Transfection was performed with Lipofectamine 2000 (Invitrogen); for co-transfections the plasmid ratio was 1 : 2 (NR1 : NR2) or 1 : 2 : 4 (NR1 : NR2 : NR3). The total amount of plasmid DNA was 1.6 µg per coverslip (calcium imaging) or 4 µg per well (cell sorting). Transfection media was replaced 4 h post-transfection with fresh culture media containing 100 µM 2-amino-5-phosphonopentanoic acid (APV) to prevent NMDA receptor-mediated excitotoxicity (Anegawa *et al.* 1995).

Ca²⁺-imaging

Twenty-four hours post-transfection cells were loaded with 5 µM fura-2AM in modified Ringer's solution (135 mM NaCl, 5.4 mM KCl, 1.8 mM CaCl₂, 10 mM glucose, 5 mM HEPES, pH 7.2, 300 mOsm) + 1% bovine serum albumin and 0.025% pluronic acid (30 min at 37°C) and mounted in a perfusion chamber (Warner Instruments, Hamden, CT, USA). Cells were continuously perfused (1–2 mL/min) and chamber temperature was maintained at 37°C with a flow-through feedback tubing heater (Warner Instruments) and a feedback objective heater (Biopetechs, Butler, PA, USA); see Thomas *et al.* (2004) for more details. Before the experiments, 2-amino-5-phosphonopentanoic acid (APV) (present in the cell culture media) was removed by perfusing the cells with Ringer's solution for at least 5 min. Initial images of CFP, YFP and mCherry were collected and cells selected on the basis of the expression of the fluorescent tags (Figure S1). Cells were illuminated at 340 and 380 nm via monochromator (Cairn Research, Faversham, UK) and images were collected at 520 nm. Image acquisition rate (340/380 pair) was 1 per second during the stimulus (and the following min) and 1 per 10 seconds during wash-out. A standard 340/380 ratio versus free [Ca²⁺] calibration plot was generated ($R^2 = 0.9997$) to convert fluorescence ratio values to [Ca²⁺]_i (Calcium calibration kit; Invitrogen).

Cell-sorting

Cells were gently removed from the plates with PBS + EDTA (2 mM), washed three times with PBS and incubated on ice for 10 min with 3% bovine serum albumin in PBS + EDTA. An anti-GFP (Green Fluorescent Protein) Alexa Fluor 647-conjugated antibody (#A-31852; Invitrogen) was then added to the final concentration of 1 ng/µL and cells were incubated for 30 min. Cells were washed thoroughly before proceeding to cell sorting in a FACScaria II flow cytometer (Becton Dickinson, Franklin Lakes, NJ, USA). Cells were kept on ice at all times to prevent receptor

internalization. The anti-GFP recognizes both NR1-CFP and NR2A-YFP and these epitopes are exposed outside the cell surface. The antibody does not recognize mCherry nor will label intracellular NR1-CFP and NR2A-YFP (data not shown).

Statistics

Data are presented as mean \pm SEM and significance is determined using ANOVA or *t*-test with an appropriate *post hoc* analysis (Prism; Graphpad Software Inc., San Diego, CA, USA).

Results

NMDA receptor expression in rat brain and optic nerve

NMDA receptor expression was analysed by RT-PCR in P10 rat optic nerve and brain (Fig. 1a). The optic nerve is a CNS white matter tract composed mainly by axons and glia and thus a good model to study NMDA receptor expression in a native tissue (Salter and Fern 2005). NR1, NR2A-B and NR3A-B mRNAs were detected in both these tissues confirming expression of NMDA receptor in rodent white matter (Salter and Fern 2005). NR3B was not detected in our previous studies in mice but showed robust expression in rat,

possibly due to improved design of the primers used to detect this subunit. Although all PCR primer pairs were designed to yield only one product, amplification of a short portion of the NR3B transcript resulted in two products: one of 120 bp, as expected and an unexpected band of 280 bp particularly prominent in the optic nerve (Fig. 1a). Both bands were cloned and sequenced revealing that the 280 bp product was due to retention of intron 6. A no-RT PCR control excluded the possibility of DNA contamination (data not shown). This suggests that NR3B pre-mRNA undergoes alternative splicing in the brain and optic nerve.

NR3B undergoes alternative splicing

We then addressed the complexity of NMDA receptor transcripts. To do so, we designed primers to amplify the open reading frame of each NMDA receptor gene (Fig. 1b). The full-length mRNA of NR1, NR2B, NR2C, NR3A and NR3B were successfully amplified and cloned (Fig. 1b). NR2A and NR2D were amplified and cloned from brain mRNA (data not shown) but we failed to amplify these subunits in the optic nerve. NR1 has eight known splice isoforms because of alternative splicing of exons 5, 20, 21

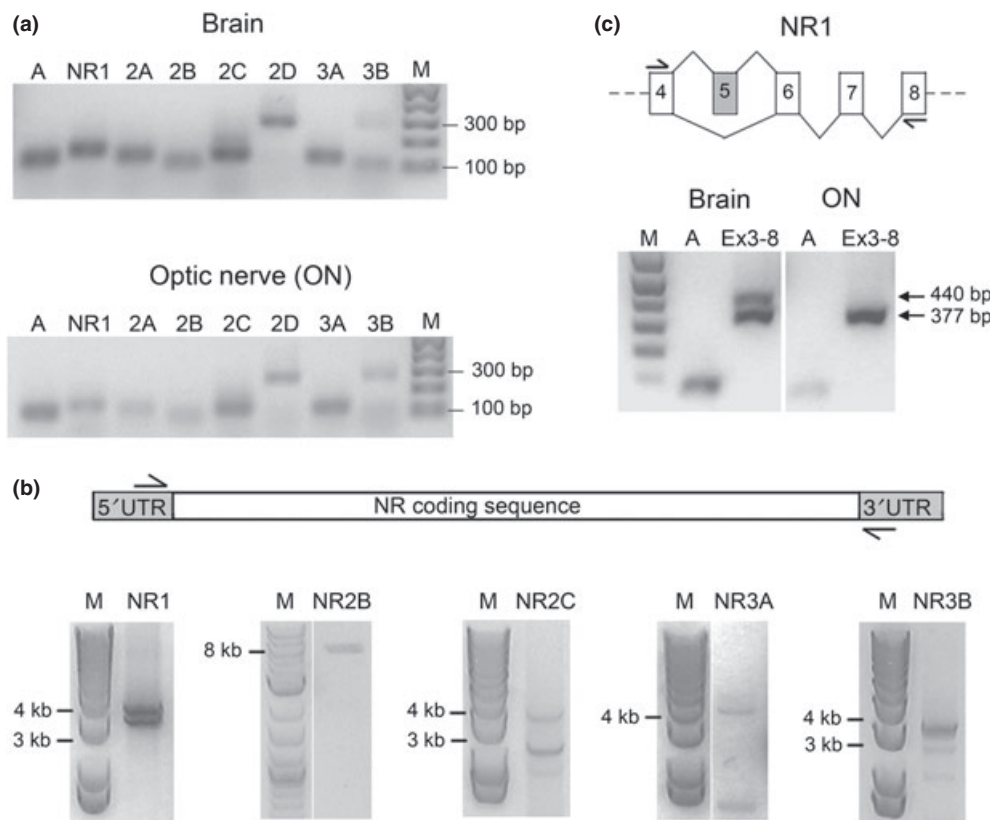


Fig. 1 NMDA receptor mRNA expression in neonatal (P10) optic nerve. (a) NMDA subunit expression in the brain and optic nerve was detected by RT-PCR. Products for all NMDA receptors splicing variants are expressed in both tissues. The primers used are listed in Table S2. Molecular weight markers are shown to the right and actin

control ('A') to the left. (b) Cloning of NMDA receptor subunits from the neonatal optic nerve. Primers were set in the UTRs of the mRNA (top, Table S3). (c) Exon 5 inclusion in NR1 mRNA was probed in the neonatal brain and optic nerve with primers running from exon 4 to exon 8 (top, Table S3).

and 22 (Sugihara *et al.* 1992; Hollmann *et al.* 1993). Clones from the optic nerve contained each of the C-terminal variations but lacked exon 5 (NR1-1a, NR1-2a, NR1-3a and NR1-4a). As exon 5 was present in clones isolated from the brain, we inquired whether exon 5 is selectively excluded in the neonate rat optic nerve. A region spanning NR1 exon 5 was amplified in both brain and the optic nerve (Fig. 1c) revealing that NR1 splice isoforms containing exon 5 are not expressed in the optic nerve at this developmental stage.

As expected (Fig. 1a, lanes 3B), amplification of NR3B mRNA yielded several products (Fig. 1b, NR3B). Sequencing of the clones revealed the previously described canonical NR3B isoform (NM133308.2), henceforth referred to as NR3B_{can} and five new variants resulting from alternative

splicing. The variant with the retained intron 6 also contained another retained intron (intron 5) and a 153 nt deletion in exon 3 (Fig. 2b, NR3B_{in5/6}). Four other NR3B isoforms were identified, containing different deletions in the coding region (Fig. 2): NR3B_{Δ24} and NR3B_{Δ45}, resulting from 24 and 45 nt deletions in the 5' of the coding sequence, respectively; NR3B_{Δ600} and NR3B_{Δ1125}, resulting from 600 and 1125 nt in the 3', respectively (Fig. 2). NR3B_{Δ600} and NR3B_{Δ1125} were cloned only from the neonate optic nerve, NR3B_{Δ24} was cloned from the neonate optic nerve and the brain and NR3B_{Δ45} was cloned only from the neonate brain. Whereas the NR3B_{Δ24} and NR3B_{Δ45} isoforms do not appear to delete important motifs, in NR3B_{Δ600} one membrane domain (M4) and in NR3B_{Δ1125}, three membrane domains are absent (Fig. 3). All the deletions were in frame, with the exception

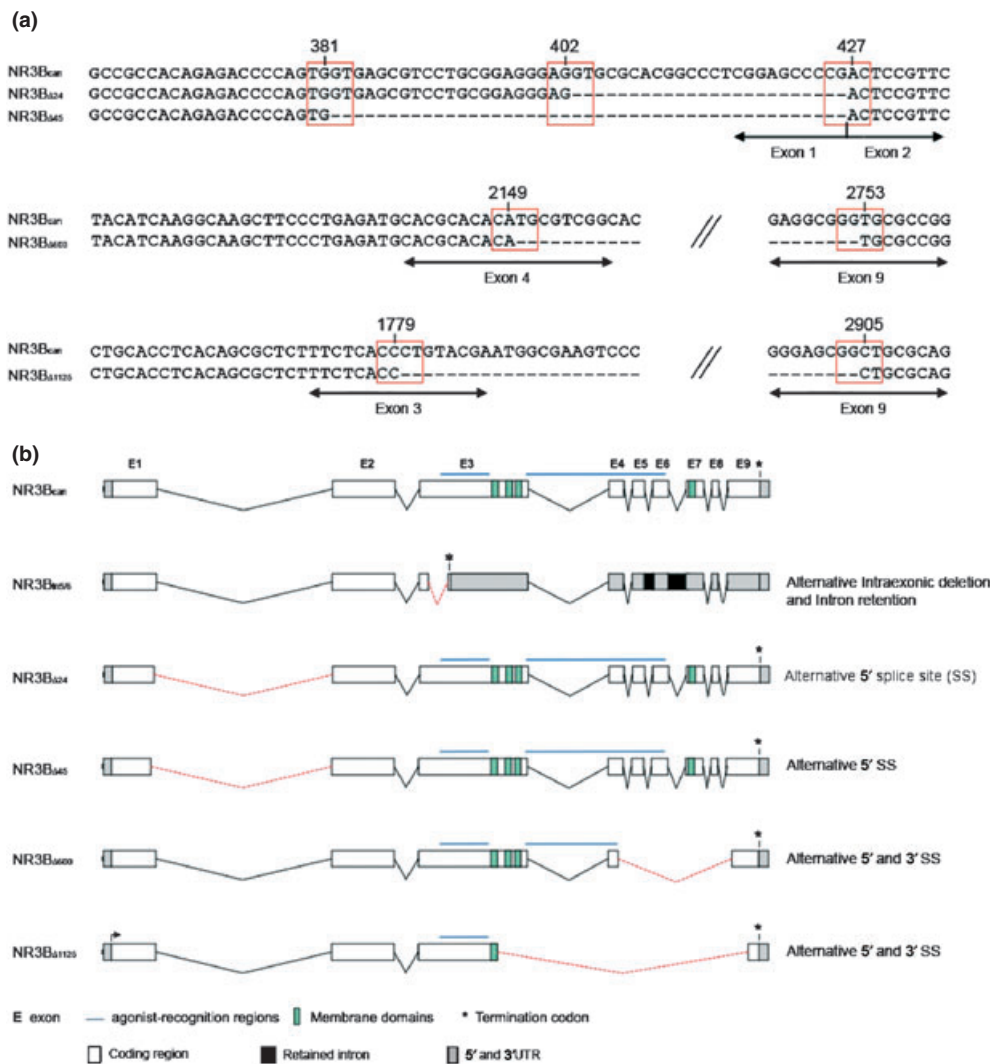


Fig. 2 Identification of five new alternative splicing isoforms of NR3B. (a) Overview of the genomic structure of the rat NR3B gene showing the location of alternative splicing events that generate the NR3B splicing isoforms. Black boxes indicate retained introns and

red dotted lines indicate deletions (as compared to the reference NR3B mRNA) (b) cDNA alignment of four of the newly identified NR3B isoforms showing the splice junctions (highlighted by the red boxes).

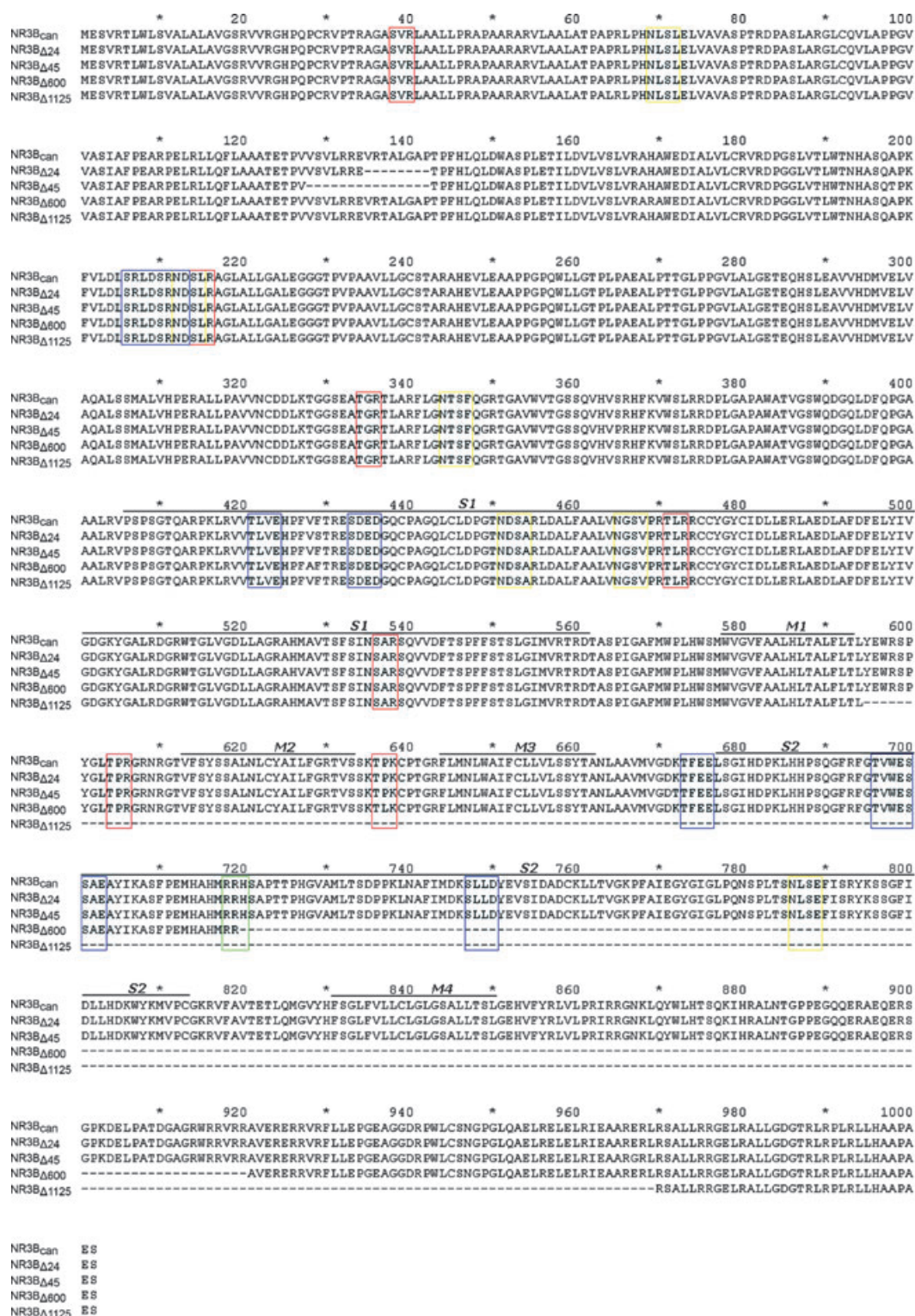


Fig. 3 Amino acid sequence alignment of the NR3B isoforms. The deduced polypeptide sequences of NR3B_{can}, NR3B_{Δ24}, NR3B_{Δ45}, NR3B_{Δ600} and NR3B_{Δ1125} were aligned using the software GeneDoc (<http://www.nrbc.org/gfx/genedoc/>). Putative sites are shown for glycosylation (yellow boxes) and phosphorylation by protein kinase C (red boxes), Ca²⁺/calmodulin-dependent protein kinase II (green

boxes) and tyrosine kinase (blue boxes) as analysed by PROSITE. The putative phosphorylation sites were also assessed for strength using NetPhos2.0 (<http://www.cbs.dtu.dk/services/NetPhos/>). Only sites with high scores are listed. Bars show the three membrane-spanning domains (M1, M3, M4), the reentrant loop (M2) and ligand binding domains (S1 and S2).

of NR3B_{in5/6}, suggesting that they encode functional proteins. All cloned variants are depicted in Fig. 2 and the alignment of the putative a.a. sequences is in Fig. 3.

Expression of NR3B isoforms changes NMDA receptor-mediated intracellular calcium $[Ca^{2+}]_i$ influx

As NR3B isoforms contain deletions that could cause major changes to NMDA receptor activity, we characterized four of these isoforms (NR3B_{Δ24}, NR3B_{Δ45}, NR3B_{Δ600} and NR3B_{Δ1125}) by recombinant expression with NR1 and NR2 subunits. The alternative intraexonic deletion occurring in NR3B_{in5/6} alters the mRNA reading frame and new in-frame early stop codons are introduced (Fig. 2b). The appearance of premature stop codons far from the canonical stop codon and/or alternative intron inclusion is considered to be a mark for mRNA degradation (Maquat 2004). Thus, we decided not to express NR3B_{in5/9}. NMDA receptor subunits were tagged with either CFP (NR1), YFP (NR2A-C) or mCherry (NR3A and NR3B isoforms) to allow visualization of cells transfected with NMDA receptors.

Cells expressing NR3B_{can}, NR3B_{Δ24}, NR3B_{Δ45}, NR3B_{Δ600} and NR3B_{Δ1125} in combination with NR1/NR2A, NR1/NR2B or NR1/NR2C were challenged with increasing concentrations of glutamate in the presence of 10 μM glycine, in Mg²⁺-free solution (Fig. 4). Under these conditions, all subunit combinations showed intracellular calcium ($[Ca^{2+}]_i$) rises upon stimulation (Fig. 4, left panels). The peak increase in $[Ca^{2+}]_i$ following stimulation was then quantified to determine the effects of NR3 expression on NMDA receptor activity. Co-expression of NR1/NR2A resulted in concentration-dependent rises in $[Ca^{2+}]_i$ evoked by perfusion with glutamate (+ 10 μM glycine/zero-Mg²⁺) and inclusion of any of the NR3 isoforms resulted in a reduction in peak amplitude of the $[Ca^{2+}]_i$ response to all glutamate concentrations tested (Fig 4a). Although expression of NR3B_{Δ45} reduced the peak of NR1/NR2A $[Ca^{2+}]_i$, this effect was smaller than NR3B_{can} in the presence of higher glutamate concentrations (Fig. 4a, 100 and 1000 μM glutamate). Expression of NR3B_{can} increased the $[Ca^{2+}]_i$ peak of NR1/NR2B in the presence of 0.1 and 10 μM glutamate. NR3B_{Δ24} and NR3B_{Δ600} also increased the $[Ca^{2+}]_i$ peak of NR1/NR2B (Fig. 4b, 1–100 μM glutamate). In contrast, $[Ca^{2+}]_i$ peak of NR1/NR2B was reduced by the expression of NR3B_{Δ1125} (Fig. 4b, all concentrations). Although no NR3B isoform significantly affected the amplitude of responses in NR1/NR2C receptors (Fig. 4c), all the NR3B isoforms reduced the number of cells from which measurable $[Ca^{2+}]_i$ were observed (Figure S2). This was not seen in other receptor subunit combinations (Figure S2) and possibly reflected reduced $[Ca^{2+}]_i$ rises in these cells to below the limit of detection. Nevertheless, NR3A expression increased NR1/NR2C $[Ca^{2+}]_i$ peak in the presence of 10–1000 μM glutamate (Fig. 4c).

NR3B isoforms reduce NR1/NR2A cell-surface expression

NR3B mutants lacking amino acids 952–985 impair NR1 cell-surface expression (Matsuda *et al.* 2003) and fail to be targeted to the cell surface (Wee *et al.* 2000). As NR3B_{Δ1125} lacks part of this sequence (a.a. 952–969, Fig. 3) the dominant-negative effect of this isoform on NR1/NR2A (Fig. 4a) could be due to a decrease in the population of cell-surface receptors. To test this, we labelled live-transfected cells with an anti-GFP antibody to detect NMDA receptor complexes at the cell surface and quantified cell surface expression by FACS (Fig. 5). The NR1 and NR2A constructs contain the fluorescent tag in their N-terminus (Qiu *et al.* 2005), which should be exposed at the cell-surface when receptors are expressed. Thus, in non-permeabilizing conditions the anti-GFP antibody will label only NR1/NR2A complexes that are inserted in the plasma membrane (Fig. 5a). This allow us to test if the observed changes in $[Ca^{2+}]_i$ in NR1/NR2A with the NR3B variants (Fig. 4a) are a consequence of changes in the NMDA receptor population at the cell surface. NMDA receptor expression was detected and expression of NR3B isoforms did not affect the total amount of NR2A-YFP present in the cells (Fig. 5b). Incubation with the anti-GFP antibody lead to strong labelling of cells expressing NR1/NR2A compared with untransfected cells (Fig. 5c and d). Co-expression with any of the NR3B isoforms leads to a decrease in cell surface labelling of NMDA receptors, with all NR3B isoforms having a similar effect (Fig. 5d). Thus, dominant-negative effects on glutamate responses may be partially explained by decreased NMDA receptor expression at the cell surface but this effect does not account for differences between NR3B isoforms (Fig. 4a).

Modulation of NMDA receptor sensitivity to glutamate by NR3B isoforms

NR3B isoforms can modulate NR1/NR2A glutamate-induced $[Ca^{2+}]_i$ responses caused by decreased cell-surface availability of receptors; however, this does not account for all between NR3B isoforms. We thus tested if these differences could be accounted for by shifts in glutamate potency. NMDA receptor responses to glutamate (Fig. 4) were fitted in a dose–response curve (Figure S3) to calculate glutamate EC₅₀ (Table 1). Expression of all NR3B isoforms increased the glutamate EC₅₀ for NR1/NR2A (Table 1). NR3B_{can} and NR3B_{Δ24} expression decreased the glutamate EC₅₀ of NR1/NR2B whereas the other NR3B isoforms did not change significantly the glutamate EC₅₀ of NR1/NR2B receptors. NR3B isoforms have opposite effects on the glutamate potency of NR1/NR2C (Table 1). NR3B_{can} and NR3B_{Δ600} increased the EC₅₀ for glutamate whereas NR3B_{Δ45} and NR1/NR2C/NR3B_{Δ1125} acted on the opposite direction. NR3B_{Δ24} expression did not change NR1/NR2C glutamate EC₅₀. Co-expression of NR3A did not have a significant effect on

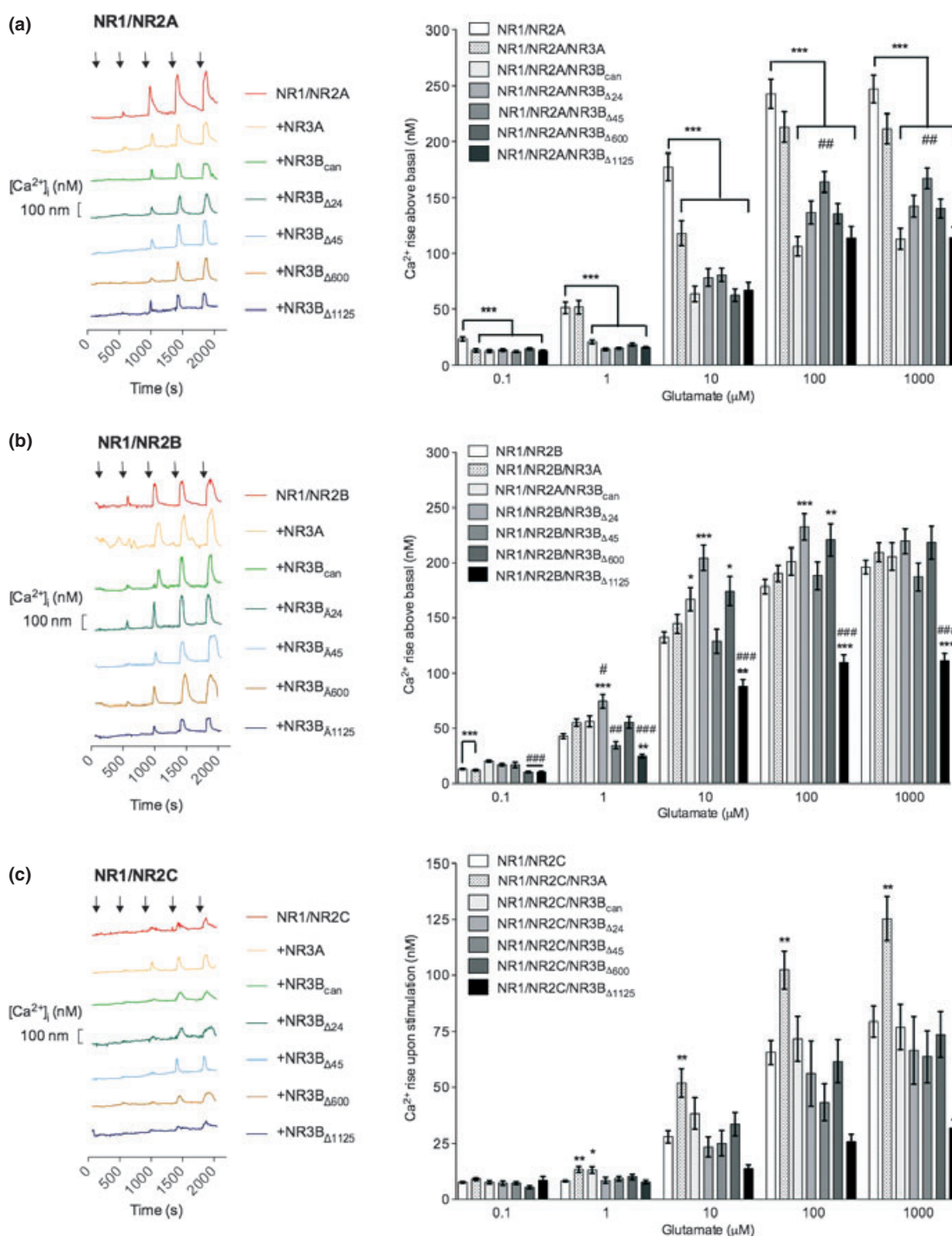


Fig. 4 NR3 subunits alter $[Ca^{2+}]_i$ rises in response to glutamate + glycine. NR1/NR2A-C were coexpressed with NR3A and NR3B isoforms and $[Ca^{2+}]_i$ changes evoked by sequential exposure to 0.1, 1, 10, 100 and 1000 μ M glutamate (15 s each, cells continually perfused with 10 μ M glycine and zero- Mg^{2+}) were recorded and quantified (right). On the left panels, each trace represents recordings from a single representative cell for each condition. Arrows indicate the time point of stim-

ulation. Each data point was obtained of 3–5 independent transfections and data are presented as mean \pm SEM. Statistical significance was accessed with one-way ANOVA with Tukey's post-test. * $p < 0.05$ versus NR1/NR2A-C alone, ** $p < 0.01$ versus NR1/NR2A-C alone, *** $p < 0.001$ versus NR1/NR2A-C alone, # $p < 0.05$ versus NR3B_{can}, ## $p < 0.01$ versus NR3B_{can}, ### $p < 0.001$ versus NR3B_{can}; number of cells per data point is 107–159 (a); 111–320 (b) and 13–126 (c).

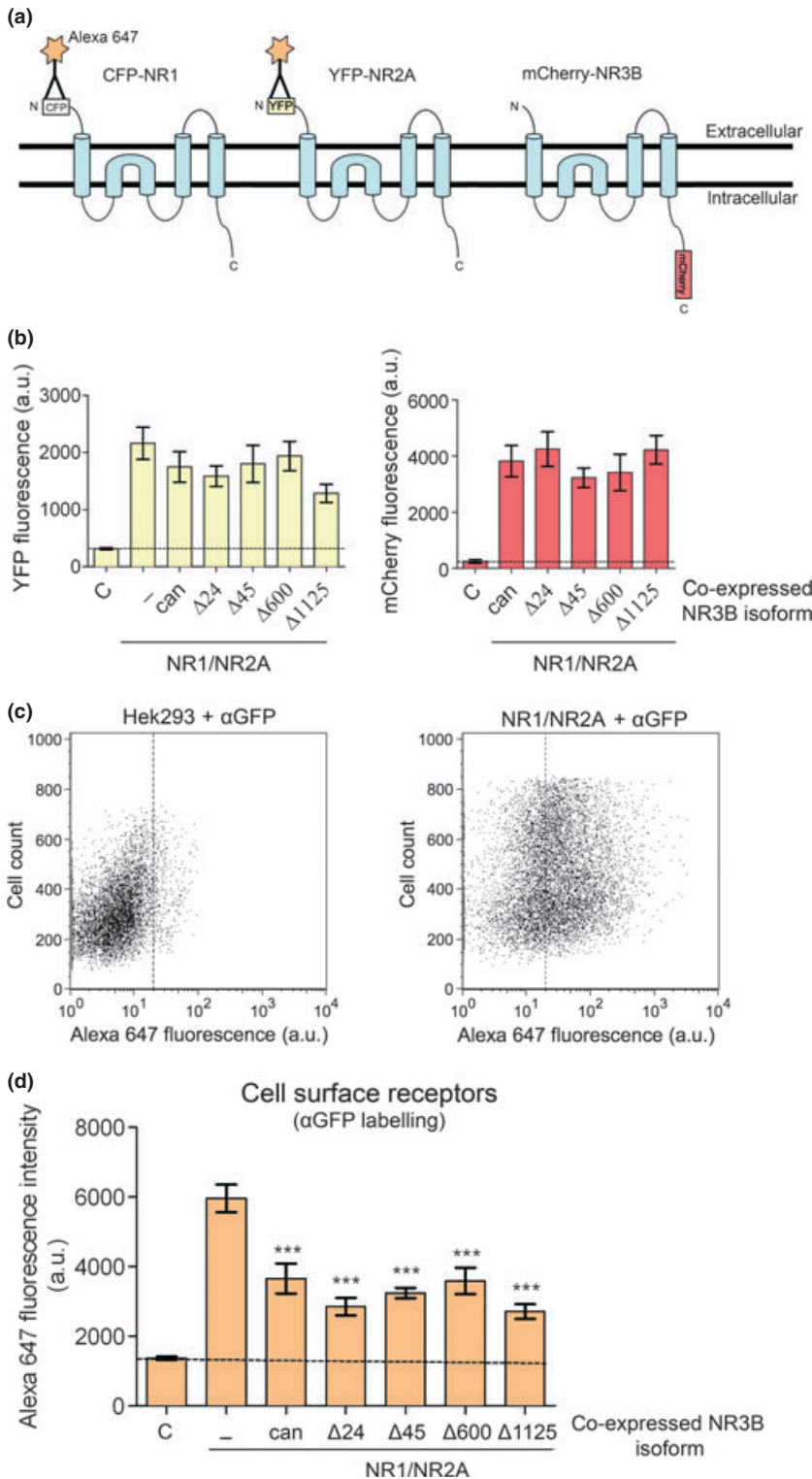


Fig. 5 Cell surface expression of NMDA receptors upon co-expression of NR3B isoforms. (a) Live cells were incubated with an anti-GFP antibody that recognizes NMDA receptor epitopes exposed extracellularly (NR1-CFP and NR2Y-YFP). (b) Total expression of NR2A and NR3B was detected due YFP and mCherry fluorescence respectively (left panel). (c) Dot plots of untransfected Hek293 and NR1/NR2A transfected cells incubated with an anti-GFP antibody labelled with alexa-647. (d) Cell-surface labelling of cells expressing the NR3B isoforms with NR1/NR2A. Data are presented as mean ± sem of fluorescence intensity (arbitrary units). Statistical significance was accessed with one-way ANOVA with Tukey's post-test. ****p* < 0.001 versus, NR1/NR2A. Data were obtained from six independent transfections. As a control column "C" in panels b and d, untransfected HEK293 cells were subjected to the same labelling procedure as transfected cells to determine non-specific labelling of the antibody. Transfection with any of the subunits combinations showed significantly higher NMDA receptor cell-surface expression versus control (d).

the glutamate EC₅₀ of either NR1/NR2A or NR1/NR2B (Table 1) but increased NR1/NR2C glutamate EC₅₀. These data indicate that expression of NR3B receptor alternative isoforms may potentially modulate NMDA receptor function in the brain and in the optic nerve.

NMDA receptor Mg²⁺-block is affected by expression of NR3B isoforms

One of the most important features of NMDA receptors is voltage-dependent block by Mg²⁺ and this block can be modulated by NR3 subunits in an NR3- and NR2-dependent

Table 1 pEC₅₀ values were estimated using glutamate dose-response curves (Figure S2) generated by single-cell Ca²⁺ imaging. Data are represented as mean ± SEM. Each data point was obtained from at least three independent transfections. Number of cells per data point is 107–159 (a); 111–320 (b) and 13–126 (c). Statistical significance was assessed with one-way ANOVA with Tukey's post-test

	pEC ₅₀	EC ₅₀ (μM)	Hill slope
NR1/NR2B	5.30	4.99	0.89
NR1/NR2B/NR3A	5.37	4.28	0.82
NR1/NR2B/NR3B	5.56 ^a	2.74	1.06
NR1/NR2B/NR3B _{Δ24}	5.69 ^b	2.03	1.20
NR1/NR2B/NR3B _{Δ45}	5.30	5.01	1.09
NR1/NR2B/NR3B _{Δ600}	5.51	3.11	1.12
NR1/NR2B/NR3B _{Δ1125}	5.44	3.65	1.23
NR1/NR2A	5.38	4.167	1.02
NR1/NR2A/NR3A	5.19	6.46	0.87
NR1/NR2A/NR3B	5.08 ^a	8.35	0.98
NR1/NR2A/NR3B _{Δ24}	5.03 ^c	9.28	1.32
NR1/NR2A/NR3B _{Δ45}	4.96 ^b	11.05	1.51
NR1/NR2A/NR3B _{Δ600}	4.90 ^b	12.55	1.30
NR1/NR2A/NR3B _{Δ1125}	5.09 ^a	8.20	1.32
NR1/NR2C	4.67	21.48	1.01
NR1/NR2C/NR3A	4.61 ^{b,d}	24.48	0.85
NR1/NR2C/NR3B	4.99 ^b	10.19	1.07
NR1/NR2C/NR3B _{Δ24}	4.65 ^d	22.56	1.16
NR1/NR2C/NR3B _{Δ45}	4.58 ^{b,d}	26.47	0.79
NR1/NR2C/NR3B _{Δ600}	4.87 ^{b,d}	13.52	0.94
NR1/NR2C/NR3B _{Δ1125}	4.48 ^{b,d}	33.53	0.95

pEC₅₀ values were estimated using glutamate dose-response curves (Fig. S2) generated by single-cell Ca²⁺ imaging. Data are represented as mean ± SEM. Each data point was obtained from at least three independent transfections. Number of cells per data point is 107–159 (a); 111–320 (b) and 13–126 (c). Statistical significance was assessed with one-way ANOVA with Tukey's post-test.

^bp < 0.001 compared to the corresponding NR1/NR2 (A-C).

^dp < 0.001 compared to NR1/NR2 (A-B)/NR3B.

manner (Sucher *et al.* 1995; Nishi *et al.* 2001; Sasaki *et al.* 2002; Yamakura *et al.* 2005). Importantly, NMDA receptor currents recorded from oligodendrocytes appear to be relatively insensitive to block by Mg²⁺ (Karadottir *et al.* 2005). We therefore sought to evaluate (i) how NR3 subunits modify Mg²⁺ block of NR1/NR2 subunits using standard experimental parameters for better comparison; (ii) whether the NR3B isoforms modulate this property of NMDA receptors. It should be noted that HEK293 cells have the same resting membrane potential, -40 mV, as myelin-forming oligodendrocytes in the P10 rat optic nerve, allowing direct comparison with results obtained in oligodendrocytes (Thomas and Smart 2005; Bolton and Butt 2006). The [Ca²⁺]_i peak evoked by activation of NR1/NR2A receptors with 100 μM glutamate (+ 10 μM glycine) was progressively reduced by increasing the extracellular Mg²⁺ from 0 to 2 and then 10 mM, an effect that was potentiated

by inclusion of any of the NR3B isoforms (Fig. 6a). NR3A had no effect on the degree of Mg²⁺-block compared with NR1/NR2A alone. Inclusion of the NR3A subunit with NR1/NR2B relieved Mg²⁺-block, whereas NR3B_{can} increased the Mg²⁺-sensitivity of the receptor (Fig. 6b). None of the NR3 subunits had any significant effect upon Mg²⁺-block of NR1/NR2C receptors (Fig 6c). The new NR3B isoforms broadly followed the same effects as NR3B_{can} (Fig. 6a–c).

Discussion

Glial expression of NMDA receptors has been reported in both astrocytes (Schipke *et al.* 2001; Lalo *et al.* 2006) and oligodendroglia (Karadottir *et al.* 2005; Salter and Fern 2005; Micu *et al.* 2006). Using RNA isolated from neonatal optic nerve and brain, we report that NR1 exon 5 alternative splicing is selectively regulated in white matter glia and that NR3B undergoes alternative splicing in both grey and white matter. We also show for the first time that the NR3B gene can produce four functional splicing isoforms: NR3B_{Δ24}, NR3B_{Δ45}, NR3B_{Δ600} and NR3B_{Δ1125}. When expressed in combination with NR1 and NR2 subunits, NR3B isoforms modify the glutamate-evoked peak [Ca²⁺]_i increase and glutamate potency of NMDA receptors in an NR2-dependent manner.

Significant differences exist between the effects of the isoforms on NMDA receptor properties. NR3B_{Δ45} was less effective at reducing response amplitude than other NR3 isoforms when co-expressed with NR1/NR2A, while NR3B_{Δ1125} was more effective at reducing responses in NR1/NR2B and NR1/NR2C receptors. Other combinations of the four isoforms with NR1/NR2 broadly mimicked the effects of NR3B_{can} upon response amplitude and Mg²⁺-block, with the exception of NR3B_{Δ24} which had no significant effect upon Mg²⁺-block of NR1/NR2B receptors. Both NR3B_{can} and NR3B_{Δ24} potentiated responses in NR1/NR2B receptors at glutamate concentrations close to the EC₅₀ and NR3B_{can} had a similar action upon NR1/NR2C receptors. However, NR3B_{Δ45} increased the glutamate EC₅₀ in NR1/NR2B and NR1/NR2C receptors. This complexity in the action of the NR3B isoforms suggest that alternative splicing of NR3B can act as a mechanism to fine-tune NMDA receptors properties, possibly in a similar manner to the modulatory effects of NR1 splicing (Traynelis *et al.* 1995; Rumbaugh *et al.* 2000).

The four isoforms are functional and modulated some aspect of NMDA receptor function (response amplitude, glutamate EC₅₀ and/or Mg²⁺-sensitivity). These effects cannot be explained by differences in cell-surface expression of the receptor complexes. Prior findings suggest that NR3 subunits act as dominant negatives, reducing NMDA currents by down-regulating surface expression (Hollmann *et al.* 1993; Cavara and Hollmann 2008). The increased response and reduced EC₅₀ in some subunit combinations following co-expression of NR3 subunits demonstrate that

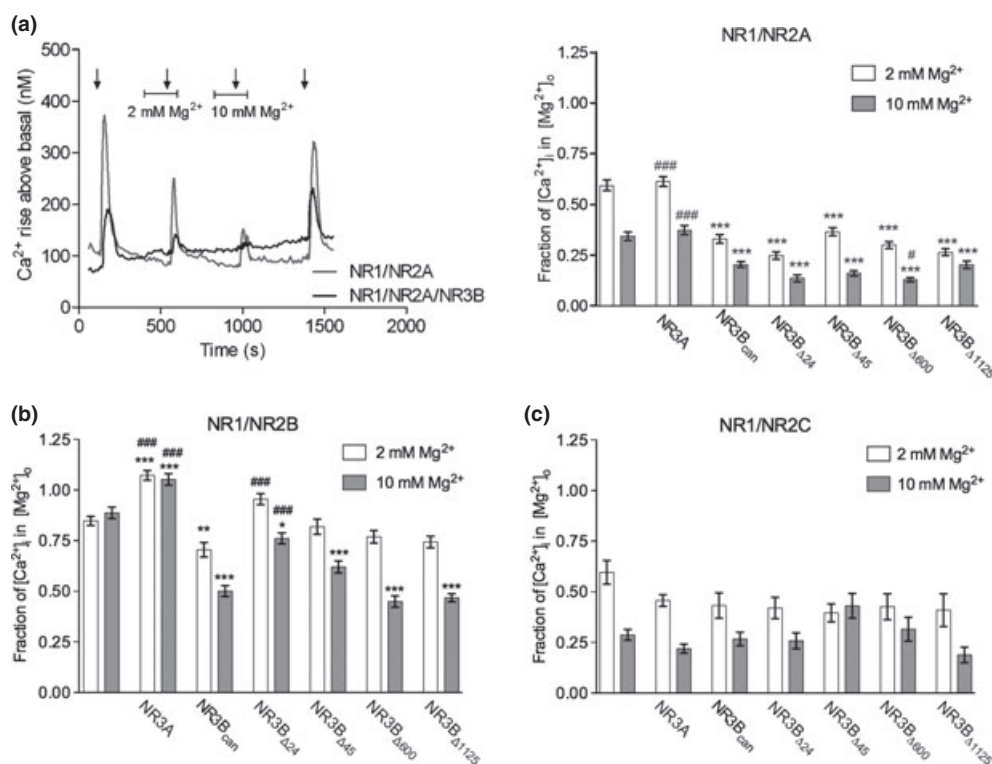


Fig. 6 The effect of NR3B isoforms on recombinant NMDA receptor Mg^{2+} -block. (a) Changes in individual NR1/NR2A and NR1/NR2A/NR3B transfected HEK293 cells exposed to 100 μM glutamate (+ 10 μM glycine) in the presence and absence of 2 and 10 mM extracellular Mg^{2+} (left). Mean $[\text{Ca}^{2+}]_i$ rises from baseline evoked by 1 mM glutamate at the two Mg^{2+} concentrations, relative to the response in Mg^{2+} -free conditions (right). (b, c) similar analysis of cells co-transfected with NR1/NR2B and NR1/NR2C respectively.

Each data point was obtained from 3–5 independent transfections and is represented as mean \pm SEM. Statistical significance was assessed with one-way ANOVA with Tukey's post-test. * $p < 0.05$ versus NR1/NR2A-C alone, ** $p < 0.01$ versus NR1/NR2A-C alone, *** $p < 0.001$ versus NR1/NR2A-C alone, # $p < 0.05$ versus NR3Bcan, ## $p < 0.01$ versus NR3Bcan, ### $p < 0.001$ versus NR3Bcan; number of cells per data point is 107–159 (a); 111–320 (b) and 13–126 (c).

dominant positive actions are also possible. Although NR3B_{Δ1125} has a partial deletion of an endoplasmic reticulum-retention signal masking motif that reduces the cell surface expression of NR1 (Matsuda *et al.* 2003), in our conditions the cell-surface availability of NR1/NR2A was not reduced upon expression of NR3B_{Δ1125} (as compared with NR3B_{can}).

NR1 exon 5 was absent from neonatal optic nerve, raising the question of whether exclusion of exon 5 is a common feature in glia. Rat Müller cells, a type of astrocytes present in the inner vertebrate retina, also predominantly express NR1 isoforms without exon 5 (Lamas *et al.* 2005). In neurons, exon 5 splicing is reversible and is controlled by activity and pH (Vallano *et al.* 1999; An and Grabowski 2007). Considering the importance of NR1 splicing in the control of NMDA receptor properties, a better appreciation of NR1 splicing in glia may help to understand the functional and pharmacological characteristics of white matter NMDA receptors under physiological and pathophysiological conditions (Karadottir *et al.* 2005; Salter and Fern 2005; Micu *et al.* 2006).

Previously, Lamas and collaborators (Lamas *et al.* 2005) have speculated that NR1a/NR2C might be the main NR1 receptor complex in Müller cells, which is consistent with data that suggests that NR2C might also be a major component of NMDA receptors in oligodendroglia (Karadottir *et al.* 2005; Salter and Fern 2005; Micu *et al.* 2006). Oligodendroglial receptors have low Mg^{2+} -sensitivity that may indicate an NR1/NR2C/NR3A stoichiometry (Sasaki *et al.* 2002; Karadottir *et al.* 2005), whereas those in cortical astrocytes are Mg^{2+} -insensitive which is inconsistent with any known subunit composition (Lalo *et al.* 2006). Although we have shown that NR3A expression increases NR1/NR2C $[\text{Ca}^{2+}]_i$ responses to glutamate, one would expect, based on the data of Karadottir *et al.* (2005), that NR1/NR2C/NR3A would have low Mg^{2+} -sensitivity. However, we found that inclusion of NR3A (or any of the NR3B isoforms) did not alter NR1/NR2C Mg^{2+} -sensitivity. An alternative explanation for the relative Mg^{2+} -insensitivity of glial NMDA receptors may reside in their location. Oligodendrocyte membrane potential is set largely by K_{ir} channels restricted to the soma (Butt and Kalsi 2006), whereas NMDA receptors

are located on the processes (Salter and Fern 2005), which may be relatively depolarized. Poor voltage command of these electrotonically distant sites may thus contribute to the low Mg^{2+} -block described in voltage-clamp experiments (Karadottir *et al.* 2005). A similar argument may explain the absence of Mg^{2+} -block of NMDA receptors in cortical astrocytes (Lalo *et al.* 2006).

NR3B receptors influence neuronal spine density and mouse behaviour (Niemann *et al.* 2007; Prithviraj and Inglis 2008) and our data highlight the potential for subtle modifications by inclusion of NR3B isoforms. NR3B_{A600} and NR3B_{A1125} were found only in optic nerve, suggesting selective expression in white matter glia. In particular, NR3B_{A1125} tended to reduce maximal responses and inclusion of this variant will produce an NMDA receptor that will mediate small $[Ca^{2+}]_i$ responses and may feasibly be suited for tonic rather than phasic signalling. One hypothesis to be addressed in the future involves the suitability of NMDA receptors incorporating this variant for the co-ordination of the morphological arrangement between axons and glia in developing white matter (Alix *et al.* 2008). The ability of NMDA receptors to mediate incidence detection corresponds with the extension and retraction of oligodendroglial processes to the axolemma during myelin initiation (Butt and Ransom 1993). Unlike incidence detection at the synapse, this is a gradual process leading to the appropriate selection of axon regions for internodal myelination. Incorporation of novel NR3B subunit variants could tailor glutamate-sensitivity, Mg^{2+} -block and Ca^{2+} permeability for this role. Inclusion of variants will also influence the injury response of oligodendroglia, in particular acting to limit toxic Ca^{2+} influx under the ischemia conditions which damage these cells during disorders such as stroke and cerebral palsy (Domingues *et al.* 2000; Alix and Fern 2009).

Acknowledgements

The authors would like to thank Minna-Liisa Änkö (MPI-CBG, Germany) for helpful discussions and comments of the manuscript, Ina Nuesslein (MPI-CBG, Germany) for technical assistance with FACS, Dr Luo (Zhejiang University School of Medicine, China) for the NMDA receptor plasmids and Dr Tsien (University of California, USA) for the mCherry plasmid. This work was supported by funds from NIH (NS44875 to RF) and the Max Planck Society (to KMN).

Declaration of interests

The authors declare no conflict of interest.

Supporting information

Additional supporting information may be found in the online version of this article:

Figure S1. Expression of tagged NMDA receptors (NR1, NR2B and NR3B) in HEK293 cells.

Figure S2. Quantification of transfected cells and responsive cells after stimulation with glutamate.

Figure S3. Glutamate dose-responses from individual cells transfected with NMDA receptors were plotted to calculate glutamate EC₅₀.

Table S1. List of PCR cycle conditions used for full-length cDNA amplification.

Table S2. List of PCR primers used for detection of NMDA receptor expression (Fig. 1a).

Table S3. PCR primers used for the detection of NR1 exon 5 (Fig. 1c).

Table S4. PCR primers used for amplification of NMDA receptor full-length cDNA amplification (Fig. 1b).

As a service to our authors and readers, this journal provides supporting information supplied by the authors. Such materials are peer-reviewed and may be re-organized for online delivery, but are not copy-edited or typeset. Technical support issues arising from supporting information (other than missing files) should be addressed to the authors.

References

- Alix J. J. and Fern R. (2009) Glutamate receptor-mediated ischemic injury of premyelinated central axons. *Ann. Neurol.* **66**, 682–693.
- Alix J. J. P., Dolphin A. C. and Fern R. (2008) Vesicular apparatus, including functional calcium channels, are present in developing rodent optic nerve axons and are required for normal node of Ranvier formation. *J. Physiol.* **586**, 4069–4089.
- An P. and Grabowski P. J. (2007) Exon silencing by UAGG motifs in response to neuronal excitation. *PLoS Biol.* **5**, e36.
- Anegawa N. J., Lynch D. R., Verdoorn T. A. and Pritchett D. B. (1995) Transfection of *N*-methyl-D-aspartate receptors in a nonneuronal cell line leads to cell death. *J. Neurochem.* **64**, 2004–2012.
- Bolton S. and Butt A. M. (2006) Cyclic AMP-mediated regulation of the resting membrane potential in myelin-forming oligodendrocytes in the isolated intact rat optic nerve. *Exp. Neurol.* **202**, 36–43.
- Butt A. M. and Kalsi A. (2006) Inwardly rectifying potassium channels (Kir) in central nervous system glia: a special role for Kir4.1 in glial functions. *J. Cell Mol. Med.* **10**, 33–44.
- Butt A. M. and Ransom B. R. (1993) Morphology of astrocytes and oligodendrocytes during development in the intact rat optic nerve. *J. Comp. Neurol.* **338**, 141–158.
- Cavara N. and Hollmann M. (2008) Shuffling the Deck Anew: how NR3 tweaks NMDA receptor function. *Mol. Neurobiol.* **38**, 16–26.
- Constantinou S. and Fern R. (2009) Conduction block and glial injury induced in developing central white matter by glycine, GABA, noradrenalin, or nicotine, studied in isolated neonatal rat optic nerve. *Glia* **57**, 1168–1177.
- Domingues A. M. d. J., Taylor M. and Fern R. (2010) Glia as transmitter sources and sensors in health and disease. *Neurochem. Int.*, **57**, 359–366.
- Gallo V., Mangin J. M., Kukley M. and Dietrich D. (2008) Synapses on NG2-expressing progenitors in the brain: multiple functions? *J. Physiol.* **586**, 3767–3781.
- Hollmann M., Boulter J., Maron C., Beasley L., Sullivan J., Pecht G. and Heinemann S. (1993) Zinc potentiates agonist-induced currents at certain splice variants of the NMDA receptor. *Neuron* **10**, 943–954.

- Ishibashi T., Dakin K. A., Stevens B., Lee P. R., Kozlov S. V., Stewart C. L. and Fields R. D. (2006) Astrocytes promote myelination in response to electrical impulses. *Neuron* **49**, 823–832.
- Karadottir R., Cavelier P., Bergersen L. H. and Attwell D. (2005) NMDA receptors are expressed in oligodendrocytes and activated in ischaemia. *Nature* **438**, 1162–1166.
- Kukley M., Capetillo-Zarate E. and Dietrich D. (2007) Vesicular glutamate release from axons in white matter. *Nat. Neurosci.* **10**, 311–320.
- Lalo U., Pankratov Y., Kirchoff F., North R. A. and Verkhratsky A. (2006) NMDA receptors mediate neuron-to-glia signaling in mouse cortical astrocytes. *J. Neurosci.* **26**, 2673–2683.
- Lamas M., Lee-Rivera I. and Lopez-Colome A. M. (2005) Cell-specific Expression of N-Methyl-D-Aspartate Receptor Subunits in Muller Glia and Neurons from the Chick Retina. *Invest. Ophthalmol. Vis. Sci.* **46**, 3570–3577.
- Low C.-M. and Wee K. S.-L. (2000) New insights into the Not-So-New NR3 subunits of N-Methyl-D-aspartate receptor: localization, structure, and function. *Mol. Pharmacol.*, **78**, 1–11.
- Maquat L. E. (2004) Nonsense-mediated mRNA decay: splicing, translation and mRNP dynamics. *Nat. Rev. Mol. Cell Biol.* **5**, 89–99.
- Marshall J., Molloy R., Moss G. W. J., Howe J. R. and Hughes T. E. (1995) The jellyfish green fluorescent protein: A new tool for studying ion channel expression and function. *Neuron* **14**, 211–215.
- Matsuda K., Fletcher M., Kamiya Y. and Yuzaki M. (2003) Specific assembly with the NMDA receptor 3B subunit controls surface expression and calcium permeability of NMDA receptors. *J. Neurosci.* **23**, 10064–10073.
- Micu I., Jiang Q. and Coderre E. *et al.* (2006) NMDA receptors mediate calcium accumulation in myelin during chemical ischaemia. *Nature* **439**, 988–992.
- Niemann S., Kanki H. and Fukui Y. *et al.* (2007) Genetic ablation of NMDA receptor subunit NR3B in mouse reveals motoneuronal and nonmotoneuronal phenotypes. *Eur. J. Neurosci.* **6**, 1407–1420.
- Nikolaeva M. A., Richard S., Mouihate A. and Stys P. K. (2009) Effects of the noradrenergic system in rat white matter exposed to oxygen-glucose deprivation in vitro. *J. Neurosci.* **29**, 1796–1804.
- Nishi M., Hinds H., Lu H. P., Kawata M. and Hayashi Y. (2001) Motoneuron-specific expression of NR3B, a novel NMDA-type glutamate receptor subunit that works in a dominant-negative manner. *J. Neurosci.*, **21**, RC185.
- Ouardouz M., Coderre E. and Basak A. *et al.* (2009a) Glutamate receptors on myelinated spinal cord axons: I. GluR6 kainate receptors. *Ann. Neurol.* **65**, 151–159.
- Ouardouz M., Coderre E., Zamponi G. W., Hameed S., Yin X., Trapp B. D. and Stys P. K. (2009b) Glutamate receptors on myelinated spinal cord axons: II. AMPA and GluR5 receptors. *Ann. Neurol.* **65**, 160–166.
- Paukert M. and Bergles D. E. (2006) Synaptic communication between neurons and NG2+ cells. *Curr. Opin. Neurobiol.* **16**, 515–521.
- Prithviraj R. and Inglis F. M. (2008) Expression of the N-methyl-D-aspartate receptor subunit NR3B regulates dendrite morphogenesis in spinal motor neurons. *Neuroscience* **155**, 145–153.
- Qiu S., Hua Y.-l., Yang F., Chen Y.-z. and Luo J.-h. (2005) Subunit assembly of N-methyl-D-aspartate receptors analyzed by fluorescence resonance energy transfer. *J. Biol. Chem.* **280**, 24923–24930.
- Rumbaugh G., Prybylowski K., Wang J. F. and Vicini S. (2000) Exon 5 and spermine regulate deactivation of NMDA receptor subtypes. *J. Neurophysiol.* **83**, 1300–1306.
- Salter M. G. and Fern R. (2005) NMDA receptors are expressed in developing oligodendrocyte processes and mediate injury. *Nature* **438**, 1167–1171.
- Sasaki Y. F., Rothe T. and Premkumar L. S. *et al.* (2002) Characterization and comparison of the NR3A subunit of the NMDA receptor in recombinant systems and primary cortical neurons. *J. Neurophysiol.* **87**, 2052–2063.
- Schipke C. G., Ohlemeyer C., Matyash M., Nolte C., Kettenmann H. and Kirchoff F. (2001) Astrocytes of the mouse neocortex express functional N-methyl-D-aspartate receptors. *FASEB J.* **15**, 1270–1272.
- Smothers C. T. and Woodward J. J. (2003) Effect of the NR3 subunit on ethanol inhibition of recombinant NMDA receptors. *Brain Res.* **987**, 117–121.
- Sucher N. J., Akbarian S. and Chi C. L. *et al.* (1995) Developmental and regional expression pattern of a novel NMDA receptor-like subunit (NMDAR-L) in the rodent brain. *J. Neurosci.* **15**, 6509–6520.
- Sugihara H., Moriyoshi K., Ishii T., Masu M. and Nakanishi S. (1992) Structures and properties of seven isoforms of the NMDA receptor generated by alternative splicing. *Biochem. Biophys. Res. Commun.* **185**, 826–832.
- Thomas P. and Smart T. G. (2005) HEK293 cell line: a vehicle for the expression of recombinant proteins. *J. Pharmacol. Toxicol. Methods* **51**, 187–200.
- Thomas R., Salter M. G., Wilke S., Husen A., Allcock N., Nivison M., Nnoli A. N. and Fern R. (2004) Acute ischemic injury of astrocytes is mediated by Na-K-Cl cotransport and not Ca²⁺ influx at a key point in white matter development. *J. Neuropathol. Exp. Neurol.*, **63**, 856–871.
- Traynelis S. F., Hartley M. and Heinemann S. F. (1995) Control of proton sensitivity of the NMDA receptor by RNA splicing and polyamines. *Science* **268**, 873–876.
- Vallano M. L., Beaman-Hall C. M. and Benmansour S. (1999) Ca²⁺ and pH modulate alternative splicing of exon 5 in NMDA receptor subunit 1. *Neuroreport* **10**, 3659–3664.
- Verkhratsky A. and Kirchoff F. (2007) Glutamate-mediated neuronal-glia transmission. *J. Anat.* **210**, 651–660.
- Wee K. S.-L., Wee Z.-N., Chow N. B.-H. and Low C.-M. (2000) The distal carboxyl terminal of rat NR3B subunit regulates NR1-1a/NR3B and NR1-2a/NR3B surface trafficking. *Neurochem. Int.* **57**, 97–101.
- Yamakura T., Askalany A. R., Petrenko A. B., Kohno T., Baba H. and Sakimura K. (2005) The NR3B subunit does not alter the anesthetic sensitivities of recombinant N-methyl-D-aspartate receptors. *Anesth. Analg.* **100**, 1687–1692.

Supplementary data

Table S1: List of PCR cycle conditions used for full-length cDNA amplification.

Subunit	Initial denaturation	40 cycles			Final amplification
		Denaturation	Annealing	Amplification	
NR1	95°C 1 min	95°C 30 sec	58°C 30 sec	68°C 8 min	68°C 10 min
NR2B	95°C 1 min	95°C 30 sec	58°C 30 sec	68°C 9 min	68°C 13 min
NR2C	93°C 3 min	93°C 30 sec	64°C 30 sec	68°C 10 min	68°C 15 min
NR3A	95°C 1 min	95°C 30 sec	58°C 30 sec	68°C 8 min	68°C 10 min
NR3B	95°C 1 min	95°C 30 sec	63°C 30 sec	68°C 8 min	68°C 10 min

Table S2: List of PCR primers used for detection of NMDA receptor expression (Fig. 1A).

Primer	Sequence (5'-3')	Sequence accession number	Position	Amplicon size (bp)
Actin for	TGCTCCTCCTGAGCGCAAGTACTC	NM031144	1071 - 1094	106
Actin rev	CGGACTCATCGTACTCCTGCTTGC	NM031144	1177 - 1154	
NR1 for	GTGTCCCTGTCCATACTCAAGT	NM017010.1	2578 - 2600	139
NR1 rev	TGAAGACCCCTGCCATGTTCTC	NM017010.1	2717 - 2696	
NR2A for	AGACCACGCCTCCGATAATC	NM012573.2	4166 - 4185	107
NR2A rev	GCCTGTGATGGCAATGAGTG	NM012573.2	4273 - 4254	
NR2B for	GCTTTCAATGGCTCCAGCAATG	NM12574.1	4734 - 4755	81
NR2B rev	CTCTCTCTCCCTCACTCAG	NM12574.1	4815 - 4796	

NR2C for	GAAGAGGTCAGCAGGGAAAC	NM012575.2	4186 - 4205	120
NR2C rev	AGTCCAGCAGGAACCAAAGC	NM012575.2	4306 - 4287	
NR2D for	CGATGGCGTCTGGAATGG	NM022797.1	2281 - 2298	259
NR2D rev	AGATGAAAACCTGTGACGGCG	NM022797.1	2540 - 2521	
NR3A for	CTCCCTCAATGTAACCTCGG	AF073379.1	3731 - 3749	121
NR3A rev	GATACTCCTCCAGCTCTGTC	AF073379.1	3852 - 3833	
NR3B for	GATCTGCTCCATGACAAGTGG	NM133308.2	2476 - 2496	98
NR3B rev	TCCTGAGAAGTGGTAGACC	NM133308.2	2574 - 2556	

Table S3: PCR primers used for the detection of NR1 exon 5 (Fig. 1C).

Primer	Sequence (5'-3')	Sequence accession number	Position	Amplicon size (bp)
<i>NR1</i>				
ex4 for	AGTCCAGCGTCTGGTTTGAG	NM_017010.1	705 - 724	377
ex8 rev	TGATGAGCTGAAGTCCGATG	NM_017010.1	1082 - 1063	

Table S4: PCR primers used for amplification of NMDA receptor full-length cDNA amplification (Fig. 1B).

Primer	Sequence	Sequence accession number	Position	Amplicon size
NR1 for	CAAACACGCTTCAGCACCTC	RNU08267	77 - 96	2880
NR1 rev	AGCAGCAGGACTCATCAGTG	RNU08267	2957 - 2938	
NR2B for	CTCTCTCCCTTAATCTGTCCG	NM12574.1	284 - 304	4531
NR2B rev	CTCTCTCTCCCTCACTCAG	NM12574.1	4815 - 4796	

NR2C for	CCCTTCCCTTCTTCTGTTTGTCCATCTACC	NM012575.2	486 - 515	3802
NR2C rev	GCTGCCAGTAACCTCACACTTCTGATTC	NM012575.2	4288 - 4261	
NR2D for	TAGCCTCATCCTTGCCTAGTCTGGTG	NM022797	447 - 472	4383
NR2D rev	CAGGTCCGTTTCTGTCCTTCCCAAC	NM022797	4830 - 4806	
NR3A for	GAGGATGTTAAGCAGAGGAGC	AF073379.1	237 - 257	3698
NR3A rev	GTGTCTCAAGGGCTTCAGAG	AF073379.1	3935 - 3916	
NR3B for	CGCACAGCACAGTGGTAACTTC	NM133308.2	47 - 68	3058
NR3B rev	ACAGTGCGGCCTTGTGGTTC	NM133308.2	3105 - 3086	

Supplementary figure 1

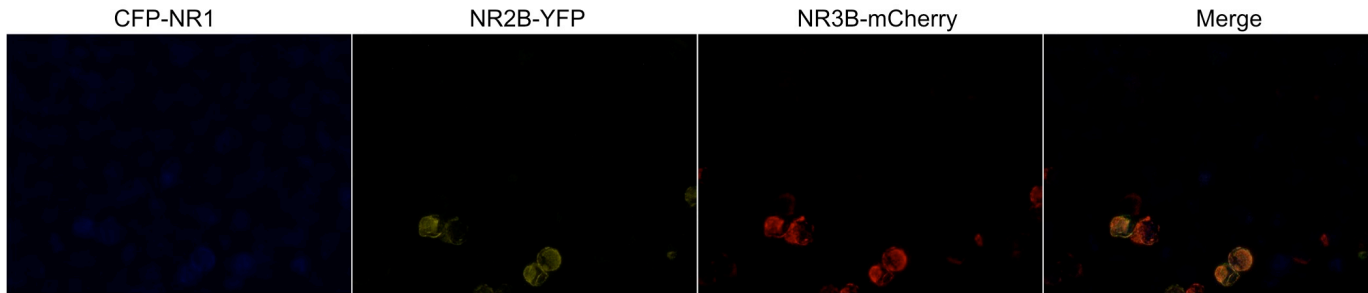


Figure S1. Expression of tagged NMDA receptors (NR1, NR2B and NR3B) in HEK293 cells.

Prior to the calcium-imaging experiments images were collected using the appropriate filters for each fluorescent protein and cells selected on the basis of expression of the fluorescent tags. As seen in Supplementary fig. 2, we were able to record significant calcium changes in more than 80% of selected cells with the exception of NR2C expressing cells. Images were acquired in a Zeiss Axioplan 2 fluorescent microscope using a 63x objective (N.A.=1.4).

Supplementary figure 2

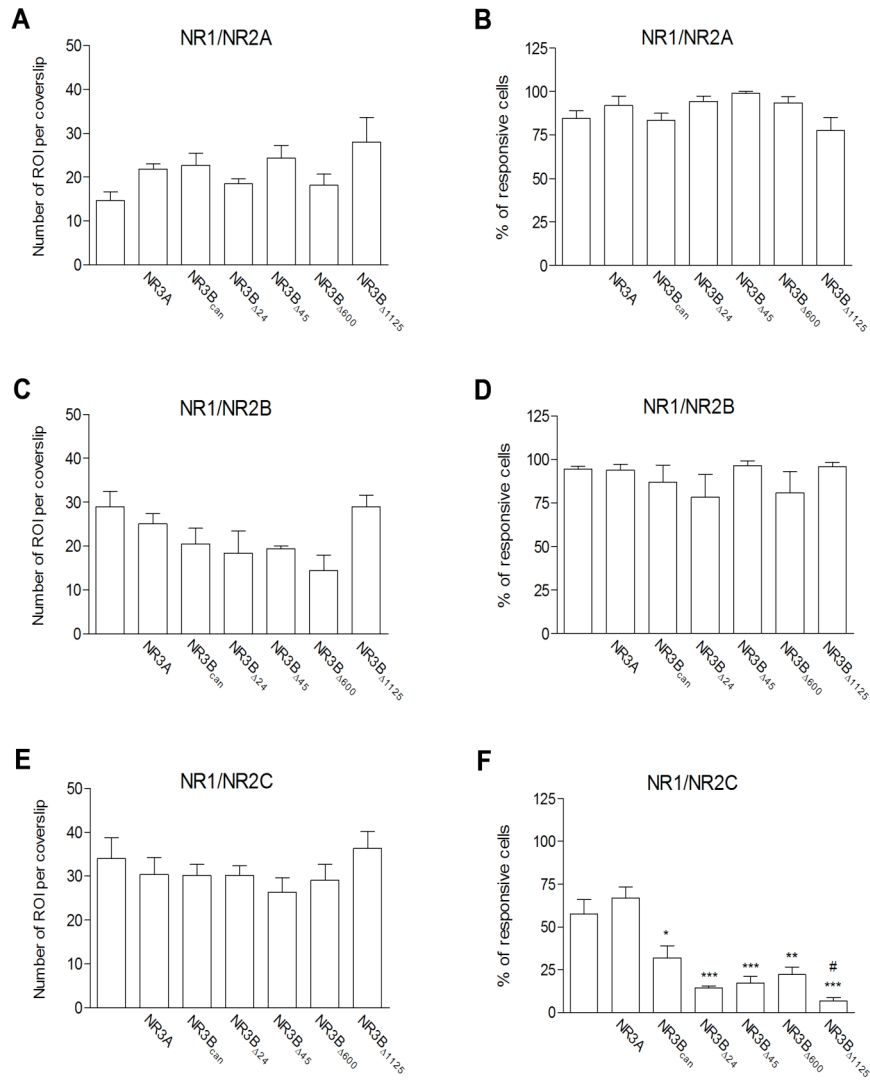


Figure S2. Quantification of transfected cells and responsive cells after stimulation with glutamate.

Although a similar number of cells express each NMDA receptor subtype (A, C and E) the percentage of cells with $[Ca^{2+}]_i$ rises above basal is smaller in NR2C expressing cells. Coexpression of NR3B variants increases this effect (B, D and F). Data is represented as mean \pm sem. Number of cells per data point is 116-205 (A); 121-342 (B)

and 174-218 (C) of at least 3 independent transfections. Statistical significance was assessed with one-way ANOVA with Tukey's post-test. * $P < 0.05$ compared to NR1/NR2C; *** $P < 0.01$ compared to NR1/NR2C; *** $P < 0.001$ compared to NR1/NR2C; # $P < 0.05$ compared to NR1/NR2C/NR3B.

Supplementary figure 3

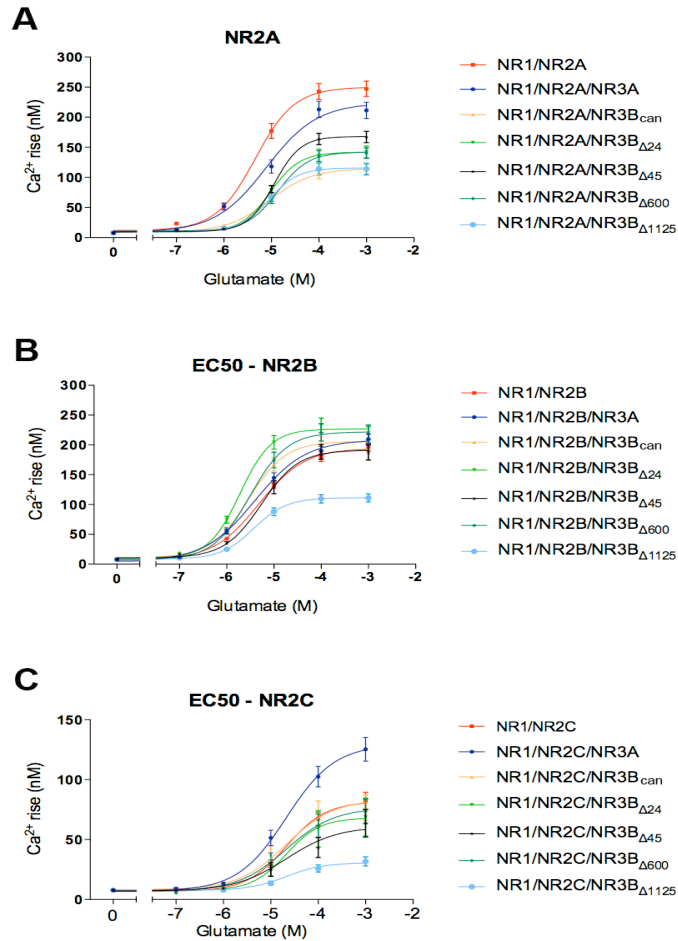


Figure S3. Glutamate dose-responses from individual cells transfected with NMDA receptors were plotted to calculate glutamate EC50.

Intracellular Ca^{2+} rises were normalized to the maximal responses (obtained with 1 mM glutamate). The calculated EC50s can be shown on figure V-3. Data is represented as mean \pm sem. Each data point was obtained of at least 3 independent transfections. Number of cells per data point is 107-159 (A); 111-320 (B) and 13-126 (C).